Journal of
Tissue Science & Engineering

Chen et al. J Tissue Sci Eng 2012, S:11
DOI: 10.4172/2157-7552.S11-003

Research Article Open Access

Collagen-Based Scaffolds for Potential Application of Heart Valve Tissue Engineering

Qi Chen[1], Arne Bruyneel[2], Kieran Clarke[2], Carolyn Carr[2] and Jan Czernuszka[1]*

[1]*Department of Materials, University of Oxford, Parks Road, Oxford, OX1 3PH, UK*
[2]*Department of Physiology, Anatomy and Genetics, University of Oxford, Parks Road, Oxford, OX1 3PT, UK*

Abstract

Collagen, glycosaminoglycans and elastin are the major components of heart valves. This work examines the roles of the composition of the collagen-based scaffolds on the microstructures, mechanical properties, and bioactivities. Scaffolds (with up to 80% elastin or 50% chondroitin-4-sulfate) were prepared by freeze drying suspensions of various compositions. The as-prepared scaffolds had mean pore sizes ranging from 115.6 μm to 187.6 μm. Mechanical characterizations showed that the scaffolds behaved as elastomers, and their characteristic mechanical properties were also dependent on the composition. The tensile, compressive, and bending modulus ranged from 39.8 ± 8.8 kPa, 10.2 ± 1.6 kPa, and 25.4 ± 5.1 kPa to 344.6 ± 42.6, 28.3 ± 4.6 kPa, and 78.3 ± 9.7 kPa, respectively. Cardiosphere derived cells were cultured on the scaffolds, and exhibited significant proliferation throughout the course of the experiment. Depending on the precise composition of the scaffold, chondroitin-4-sulfate increased the proliferation rate of the cells while elastin lowered it. The native heart valve has a tri-layer structure with the layers having compositions similar to those used in this study. Thus, the findings from this study will have implications on how to fabricate a more successful scaffold for tissue engineering heart valves.

Keywords: Collagen scaffold; Heart valve; Pore size; Mechanical property; Cardiosphere-derived cells

Introduction

Tissue engineering is a potential approach for creating additional tissues. It involves *in vitro* cell culturing on a scaffold and subsequent implantation of the cell-scaffold composite into the patient for tissue regeneration. The scaffold acts as an analogue of the extracellular matrix (ECM) of the tissue and is crucial to the tissue engineering process. It should provide a suitable micro-environment for the cells, so that there is good cell adhesion, migration, proliferation, and differentiation. Meanwhile, the scaffold also needs sufficient mechanical properties to enable the new tissue to perform normal mechanical functions.

A native heart valve (taking the aortic valve for example) consists of three distinct layers: the fibrosa is on the aorta side of the valve leaflet, with the ECM substance being predominantly collagen fibres; the ventricularis is on the ventricle side of the valve leaflet and is comprised of elastin and collagen sheets; between the fibrosa and the ventricularis is the spongiosa, which is rich in glycosaminoglycans (GAGs) and also contains loosely arranged collagen [1].

This work, therefore, investigated scaffolds with compositions resembling each layer of the native heart valve, i.e. collagen scaffolds, collagen-elastin scaffolds and collagen-GAGs scaffolds. The morphological and mechanical properties of the scaffolds were characterized. The biological properties of the scaffolds were assessed by *in vitro* culturing of cardiosphere-derived cells (CDCs). CDCs are derived from the endogenous stem cell population present in the adult heart and are able to differentiate into the cells of the three cardiac lineages [2]. Therapeutic efficacy has been established in animal models [3,4], and a clinical trial is currently on-going [5], demonstrating that CDCs are a promising candidate for heart tissue regeneration. The results of this study served as a forwarding step towards a tri-layer structure that even more closely mimics the ECM of a native heart valve.

Materials and Methods

Scaffolds preparation

Type I collagen (from bovine Achilles tendon), chondroitin-4-sulfate (C4S) (from bovine trachea) and elastin (from bovine neck ligament), were selected as scaffold materials, and were all obtained from Sigma-Aldrich Ltd, UK. Scaffolds were fabricated by freeze-drying suspensions with various compositions, as required.

For collagen and collagen-elastin scaffolds, a suspension was made with the desired weight ratio (100% collagen, 50% collagen-50% elastin, 20% collagen-80% elastin) in 0.05 M acetic acid (pH 3.2). All the suspensions were of the same total concentration of 1% wt/v.

For the collagen-C4S scaffolds, collagen was firstly suspended in acetic acid, and then the C4S was added into the suspension, instantly co-precipitating with the collagen and forming an agglomeration [6]. The agglomeration was reduced by drop-wise adding 2M sodium hydroxide solution to the suspension until the pH value reached 7 [6], resulting in a homogeneous suspension of fine collagen-C4S co-precipitates. The total concentration of the suspension was also 1% wt/v and two different compositions (90% collagen-10% C4S, 50% collagen-50% C4S) were used.

The suspension was cast into polytetrafluoroethylene (PTFE) moulds according to the required dimensions of the samples, frozen at -20C, and freeze-dried (Christ I-5, Martin Christ) for 24 hours in

***Corresponding author:** Jan Czernuszka, Department of Materials, University of Oxford, Parks Road, Oxford, OX1 3PH, UK, E-mail: jan.czernuszka@materials.ox.ac.uk

Received November 16, 2012; **Accepted** December 17, 2012; **Published** December 20, 2012

Citation: Chen Q, Bruyneel A, Clarke K, Carr C, Czernuszka J (2012) Collagen-Based Scaffolds for Potential Application of Heart Valve Tissue Engineering. J Tissue Sci Eng S11:003. doi:10.4172/2157-7552.S11-003

a vacuum of 0.05 mbar, removing the ice crystals by sublimation and leaving the porous solid scaffolds.

Scaffold mechanical properties

Unidirectional tension tests were conducted using a Rubicon tensile machine (Denison Mayes Group), and unidirectional compression and three-point bend tests were conducted using a DMA7 (PerkinElmer). All samples were tested dry at room temperature.

Rectangular samples (length: 40 mm, width: 12 mm, thickness: 5 mm) were tested in tension with a gauge length of 20 mm and a strain rate of 3%/min until rupture; and in three-point bending where the samples were loaded at a cross-head speed of approximately 0.5 mm/min with a span of 20 mm. For the compression tests, cylindrical samples of 15mm in both diameter and height were loaded at an approximately constant strain rate of 3%/min on all samples.

CDCs harvest and isolation

CDCs were isolated from adult Sprague Dawley rats (Harlan) and expanded in accordance with previously published protocols [4,7,8]. Briefly, rats were killed by lethal injection, and the hearts were explanted, washed with Dulbecco's phosphate buffered saline (DPBS; Sigma-Aldrich), and minced into small explant pieces in 0.05% trypsin-EDTA (Invitrogen). Explants were then placed on fibronectin-coated 60 mm petri dishes with 1.5 ml of complete explant medium (CEM), comprising Iscove's modified Dulbecco's medium (IMDM; Invitrogen) supplemented with 20% fetal bovine serum (FBS; Invitrogen), 1 U/ml penicillin, 1 μg/ml streptomycin and 0.2 mM L-glutamine (Gibco), and were incubated at 37°C with 5% CO_2. After approximately a week, small, round, phase bright cells grew out from the explants. Upon reaching 80-90% confluency, these explant-derived cells (EDCs) were isolated using trypsin and re-plated in poly-d-lysine-coated 24 well plates in cardiosphere growth medium (CGM) comprising 65% Dulbecco's modified eagle medium (DMEM/F12), 35% IMDM, 7% FBS, 2% B27 (Invitrogen), 25 ng/ml cardiotrophin (Peprotech EC), 10 ng/ml epidermal growth factor (EGF; Peprotech EC), 20 ng/ml basic fibroblast growth factor (FGF; Promega) and 5 units thrombin (Sigma-Aldrich). Cardiospheres formed after 2-3 days, when they were harvested by mechanical trituration and plated in CEM in fibronectin-coated flasks to culture for CDCs. EDCs could be harvested from the explants multiple times, in these experiments second and third harvest cells were used at passages three to five.

CDCs culture on scaffolds

Scaffolds (n=6 for each group) were sterilized by three 30-minute washes with 100% ethanol, followed by three 30-minute washes with DPBS. Then they were immersed in CEM in 24 well plates. CDCs (50000 cells per scaffold) were seeded on to the scaffolds and cultured for 7 days at 37°C with 5% CO_2.

Scaffold and cell morphology

Scaffold and cell morphology were characterized using scanning electron microscopy (SEM) JSM840F (JEOL Ltd) at an accelerating voltage of 4 kV. Scaffolds seeded with cells were fixed at day 7 in 4% paraformaldehyde (PFA, Sigma-Aldrich) overnight at 4°C. Samples were then dehydrated through exposure to a gradient of alcohol followed by hexamethydisilazane (HMDS, Sigma-Aldrich), and were air-dried [9]. All specimens were coated with 3 nm thick platinum by a 208HR sputter coater (Cressington Scientific Instruments Ltd) before observation. The mean pore size of the scaffolds was calculated by measuring the diameters of the pores using ImageJ (National Institutes of Health, USA).

Assessment of CDCs proliferation

CDC proliferation was assessed using the alamarBlue® assay (AbD Serotec). Measurements were taken on day 1 (20 hours after seeding, to examine cell attachment), day 4 and day 7. Briefly, the scaffolds were transferred into empty wells and washed with DPBS, and fresh CEM medium supplemented with 10% alamarBlue® was added. Scaffolds were incubated for three hours, before the supernatant was transferred into μClear black plates with a clear bottom (Greiner bio-one). Fluorescence was measured using a FLUOstar Optima plate reader (BMG Labtech) at 544/590 nm.

Statistics

All data were reported as means, with the standard deviations as the errors. One-way analysis of variance (ANOVA) followed by Tukey's test was used to compare groups of data, with a probability value of 95% ($p<0.05$) to determine statistical significance.

Results

Scaffolds microstructure characterization

Figure 1 shows the porous structures of the scaffolds with different compositions. The measured mean pore sizes of the scaffolds are listed in table 1.

Microstructure characterization found that all the scaffolds possessed approximately equiaxial pores (Figure 1). The pore size of the scaffold was observed to increase with the addition of elasin and to decrease with the addition of C4S. It can be seen on the images of individual pores (Figure 1) that with the decrease of the overall volume fractions of collagen in the scaffolds, the pore walls became thinner and more porous.

Scaffold mechanical properties

Figure 2 shows representative tension and compression stress-strain curves of a scaffold. The scaffolds exhibit behaviours typical of elastomers under tension and compression, viz. the stress-strain curves were characterized by the distinctive deformation stages [10]. In tension, the stress-strain curve had a linear elastic stage dominated by pore edge bending, and a stiffened stage due to pore wall alignment. In compression, there were three characteristic deformation stages, the first of which was also a linear elastic stage (dominated by pore edge bending), followed by a stress plateau (dominated by pore wall buckling) and densification (dominated by pore collapse throughout the scaffold) [10]. The slopes of the initial linear stages on the curves represent the tensile and compressive moduli E_{ten} and E_{comp} (Figure 2). Figure 3 shows a typical load-deflection curve of a scaffold in three-point bending test. The effective bending modulus (E_{bend}) of the scaffold was calculated from the initial slope ($\delta P/\delta D$) of the load-deflection curve, with the equation $Ebend = \left(\frac{\delta P}{\delta D}\right)\frac{l^3}{48I}$, where P is the load, D is the deflection, l is the span distance, and I is the second moment of area. The complete results of mechanical properties are presented in figure 4.

Each of the mechanical properties decreased with the decrease of the proportion of collagen in the scaffolds (Figure 4). For the scaffolds with the same composition, E_{ten} was between 4-27 times greater than E_{comp}, with E_{bend} having intermediate values.

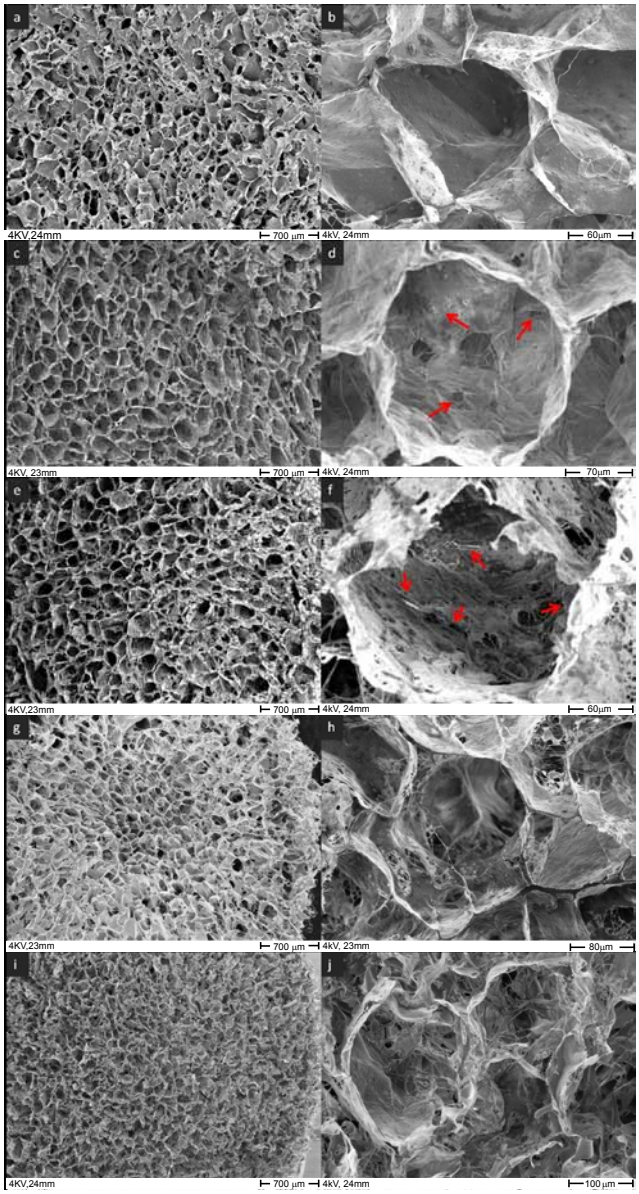

Figure 1: SEM micrographs of scaffolds with various compositions: (a, b) 100% collagen, (c, d) 50% collagen-50% elastin, (e, f) 20% collagen-80% elastin, (g, h) 90% collagen-10% C4S, (i, j) 50% collagen-50% C4S. Arrows denote elastin.

Composition	Pore Size (µm)
100% Collagen	147.6 ± 38.4
50% Collagen-50% Elastin	179.9 ± 35.8[a]
20% Collagen-80% Elastin	187.6 ± 36.5[a]
90% Collagen-10% C4S	115.6 ± 27.6[b]
50% Collagen-50% C4S	116.8 ± 17.8[b]

Table 1: Pore sizes of scaffolds with various compositions.

[a]Denotes pore sizes larger than collagen scaffolds ($p<0.05$).
[b]Denotes pore sizes smaller than collagen scaffolds ($p<0.05$).

Behaviour of CDCs on scaffolds

Figure 5 presents representative SEM images of CDCs seeded on scaffolds of different compositions. CDCs can be seen to be migrating down the interconnected pores that seem to act like miniature channels within the scaffolds for the collagen and collagen-C4S scaffolds, see figures 5a-c. This was less evident for the collagen-elastin scaffolds; see figure 5d, where the cells seemed to remain nearer the surface. This direct evidence supports the findings that cell proliferation occurs in all cases, and that increasing parts of the scaffold are colonized as time increases. Further, the composition of the scaffold is important in how cells react. Further work is now being done on this area to separate the contributory factors and these findings will be presented in a subsequent paper.

Figure 6 shows the results of alamarBlue® assays representing the numbers of cells on the scaffolds at different culture times, and Table 2 shows the proliferation of cells in terms of fold changes. CDCs had similar amount of attachment (3.56%~3.91% AB reduction) on day 1 to all the scaffolds, with an exception of the 50%collagen-50% C4S group, on which the attachment was slightly lower (2.91% AB reduction) (Figure 6). CDCs proliferated significantly on all the scaffolds (>3 folds on day 4 and >5 folds on day 7), however, it was found that the cell proliferation on the collagen-elastin scaffolds was less than that on the collagen scaffolds. In contrast, the cell proliferation was greater on the collagen-C4S scaffolds.

Discussion

The pore sizes of all the scaffolds fell in the range of 100~200 µm,

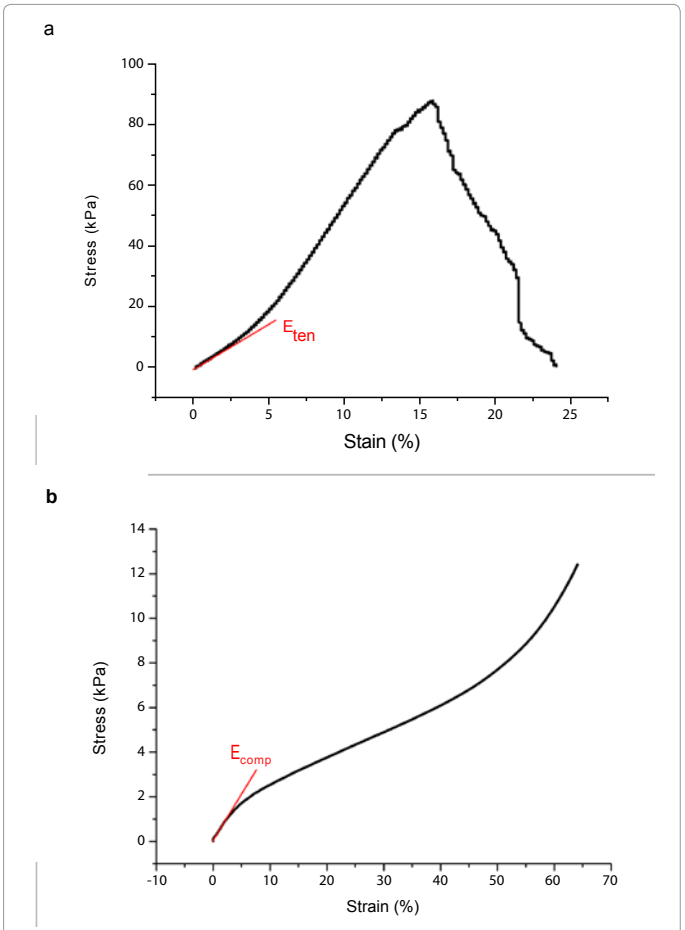

Figure 2: Unidirectional (a) tension and (b) compression stress-strain curves of 100% collagen scaffolds.

which is sufficient for exchange of oxygen and nutrients [11], and suitable for cell attachment [12]. It appears that the presence of elastin increased the pore sizes of the scaffolds. This is because the elastin does not form continuous sheets as collagen does, but is only embedded in the collagen sheets in forms of short rods (Figures 1d and 1f). As the proportion of elastin increased, there were less collagen sheets forming the pore walls, and hence larger pores were produced. The incorporation of C4S into the scaffolds, however, seemed to decrease the pore sizes. This is likely to be due to the collagen-C4S co-precipitation effect in the suspension, which has been reported to displace the hydration envelopes from the acid-swollen collagen [6], and thereby reduce the viscosity of the suspension. Lower viscosity then causes higher freezing rate in the freezing stage, producing smaller ice crystals and therefore smaller pores in the scaffolds.

The lower moduli values of the scaffolds containing elastin and C4S are due to elastin and GAGs having a much lower stiffness than collagen. Gosline reported an elastic modulus of ~1 MPa for elastin versus ~1 GPa for collagen [13], and Redaelli determined by molecular modelling the stiffness of GAGs and collagen fibrils to be 3.1×10^{-11} N/nm and 0.75×10^{-6} N/nm respectively [14]. In addition, the elastin and C4S also interferes with the integrity of the pore walls, which gives

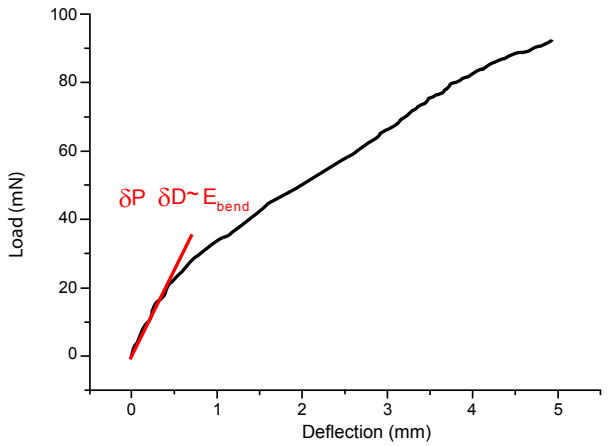

Figure 3: Load-deflection curve of three-point bend test on 100% collagen scaffold.

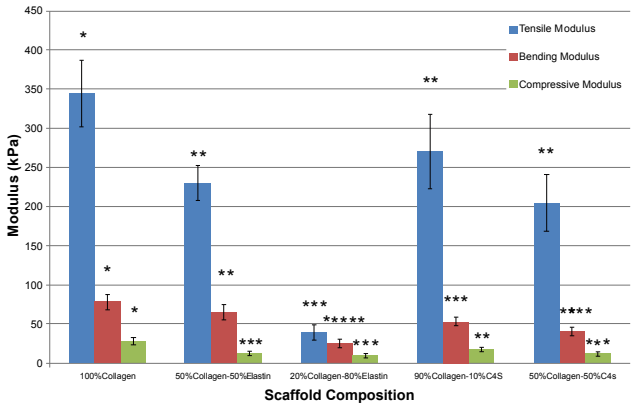

Figure 4: Average mechanical properties of scaffolds with various compositions. *, **, ***, **** and ***** denote statistical significance ($p<0.05$) amongst groups of different compositions.

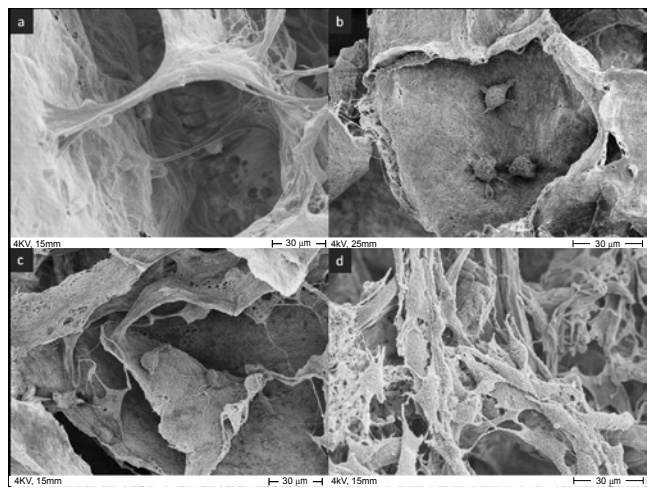

Figure 5: Scanning electron micrographs of CDCs deep within a channel in (a) 100% collagen scaffolds, (b) 90% collagen-10% C4S scaffolds, (c) 50% collagen-50% CS4 scaffolds and (d) 20% collagen-80% elastin scaffolds.

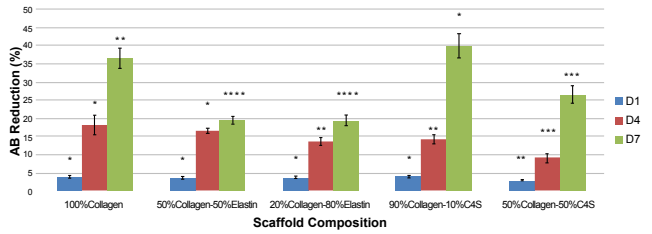

Figure 6: Proliferation of CDCs on scaffolds from day 1 to day 7. Significant cell proliferation ($p<0.05$) was found on every group of scaffolds at day 4 and day 7. *, ** *** and **** indicate statistically significant differences ($p<0.05$) amongst groups of different compositions.

Composition	D4/D1	D7/D1
100% Collagen	4.63 ± 0.32*	9.39 ± 0.86**
50% Collagen-50% Elastin	4.70 ± 0.39*	5.53 ± 0.69***
20% Collagen-80% Elastin	3.68 ± 0.30**	5.24 ± 0.36***
90% Collagen-10% C4S	3.64 ± 0.15**	10.29 ± 0.63*
50% Collagen-50% C4S	3.10 ± 0.19***	9.15 ± 0.95**

Table 2: Percentage of alamarBlue® reduction of D4 and D7 normalized to values of D1. *, ** and *** indicate statistically significant differences ($p<0.05$) amongst groups of different compositions.

the pore walls an increased porosity and hence lower inherent load-bearing abilities of the scaffolds.

For the scaffolds with the same composition, the deformation regimes of elastomeric foam mentioned above should predict equal values of E_{ten} and E_{comp}, because they are governed by the same deformation mechanism: pore edge bending. However, the tensile modulus of the scaffolds was found to be approximately one order of magnitude higher than that in compression. This can be explained by further examining the deformation mechanism of individual pores. Taking a cubic pore as an example (Figure 7), we can see that the deforming load is exerted not only vertically onto the pore edges, but also axially onto the side walls, causing their additional stretching in tension and buckling in compression (similarly mentioned by Gibson as 'beam-column interaction' [10]). As collagen fibers are far more resistant to stretching than buckling, a higher E_{ten} is then produced.

The effective bending moduli of the scaffolds were also investigated because flexure is the primary form of deformation in native heart valves. In bending, one side of the scaffold will be in tension and the other side in compression. The E_{bend} will therefore lie in between E_{ten} and E_{comp} (see Figure 4). After the initial slope (Figure 3), with a deflection of around 0.6 mm, the upper surface of the compressive region in the scaffold will reach a critical strain and start to enter the second deformation stage (Figure 2b), which will result in a decrease in the effective modulus of the compressive region, and hence a reduced effective bending modulus (i.e. a decreased load-deflection slope in figure 3.

Merryman et al. [15] reported a bending modulus of 492 kPa for porcine aortic 77. Here, taking into consideration of the effects of hydration (which will reduce the modulus of scaffold to 1/150 of the value in dry status [16]) and cell contraction (which will approximately triple the modulus [17]), the mechanical properties of the scaffolds were still much lower than that seen in a native tissue. This suggests the need for a more well-controlled structural hierarchy and a higher density of cross linking in the scaffolds.

Cells naturally bind to collagen via intergrin receptors [18], and therefore show desirable activity on collagen scaffolds. GAGs are also believed to have advantageous interactions with cells through their abilities to bind to growth factors or directly to cell surface receptors [19,20], and have been found to improve tissue growth and regeneration when incorporated into collagen scaffolds [21,22]. In particular, the GAG used in this study, C4S, is able to enhance the metabolic activities of cells [23], which may explain the increased proliferation seen on the collagen-C4S scaffolds. It is worth noting that the 50%collagen-50%C4S scaffolds had a lower attachment of cells initially, although there was a steady cell growth afterwards. There is an upper limit of C4S binding to collagen (when the binding sites on the collagen are saturated by C4S)[6], and thus a proportion of the C4S in the scaffolds may have dissolved into the culture medium during the seeding process, attracting more cells to attach to the wells and leaving fewer cells to bind to the scaffolds. Elastin, on the other hand, is less favourable to cell proliferation than collagen [24-26], due to its non-intergrin signalling pathway [25]. Therefore, the cell proliferation on the collagen-elastin scaffolds slowed after day 4. Nonetheless, the overall growth of the cells was significant on all the scaffolds, indicating that the cells show positive responses and viabilities on the collagen-based scaffolds. Having now provided an initial assessment of the effect of scaffold composition on CDC proliferation, the next step is now to combine a 100%collagen scaffold with a 90% collagen-10% C4S scaffold and a 20% collagen-80% elastin scaffold to create a tri-layered composite scaffold that, compositionally, more closely mimics the native heart valve.

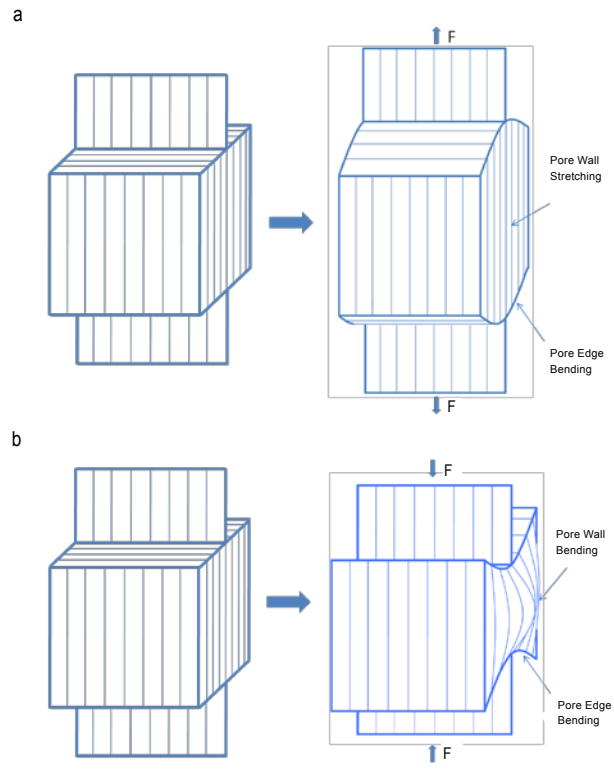

Figure 7: Schematic graphs of the deformation of an individual pore (a) in tension, and (b) in compression.

Conclusions

Collagen-based scaffolds had interconnected pore sizes ranging from 115.6 μm to 187.6 μm, and the precise value was found to depend strongly on the specific composition. Mechanical characterization suggested that the increase of elastin or C4S volume fraction lowered the moduli values of the scaffolds. The adjustable microstructures and mechanical properties bode well for the design of more complicated scaffolds in the future. Scaffolds are also responsible for mediating the signalling, growth, and metabolism of the cells. This study illustrated that cardiosphere-derived cells were able to attach to and populate the scaffolds. While C4S was found to enhance the activities of the collagen-based scaffolds for the cells, elastin showed less pronounced effects on improving the cell proliferation.

In summary, this work served as a framework of collagen-based scaffolds, by providing the information of pore size, mechanical properties, and biological properties. More importantly, it also represents a step forward from our previous work on collagen scaffolds for heart valve tissue engineering [27-29], to the final stage of a collagen-GAGs-elastin scaffold that closely resembles a native heart valve.

Acknowledgements

This study was funded by China Scholarship Council-University of Oxford Scholarship, and by a British Heart Foundation Studentship. The authors would like to acknowledge Prof. Chris Grovenor for providing the laboratory facilities.

References

1. Taylor PM, Cass AEG, Yacoub MH (2006) Extracellular matrix scaffolds for tissue engineering heart valves. Prog Pediatr Cardiol 21: 219-225.
2. Davis DR, Zhang Y, Smith RR, Cheng K, Terrovitis J, et al. (2009) Validation of the Cardiosphere Method to Culture Cardiac Progenitor Cells from Myocardial Tissue. PLoS One 4: e7195.
3. Lee ST, White AJ, Matsushita S, Malliaras K, Steenbergen C, et al. (2011) Intramyocardial Injection of Autologous Cardiospheres or Cardiosphere-Derived Cells Preserves Function and Minimizes Adverse Ventricular Remodeling in Pigs With Heart Failure Post-Myocardial Infarction. J Am Coll Cardiol 57: 455-465.
4. Carr CA, Stuckey DJ, Tan JJ, Tan SC, Gomes RS, et al. (2011) Cardiosphere-derived Cells improve function in the infarcted rat heart for at least 16 Weeks - an MRI Study. PLoS One 6: e25669.
5. Makkar RR, Smith RR, Cheng K, Malliaras K, Thomson LE, et al. (2012) Intracoronary cardiosphere-derived cells for heart regeneration after myocardial infarction (CADUCEUS): a prospective, randomised phase 1 trial. Lancet 379: 895-904.

6. Yannas IV (1992) Tissue regeneration by use of collagen-glycosaminoglycan copolymers. Clinical Materials 9: 179-187.

7. Messina E, De Angelis L, Frati G, Morrone S, Chimenti S, et al. (2004) Isolation and Expansion of Adult Cardiac Stem Cells From Human and Murine Heart. Circ Res 95: 911-921.

8. Tan JJ, Carr CA, Stuckey DJ, Ellison GM, Messina E, et al. (2007) Isolation and Expansion of Cardiosphere-Derived Stem Cells. Curr Protoc Stem Cell Biol: John Wiley & Sons, Inc.

9. Yahyouche A, Zhidao X, Czernuszka JT, Clover AJ (2011) Macrophage-mediated degradation of crosslinked collagen scaffolds. Acta Biomater 7: 278-286.

10. Gibson LJ, Ashby MF (1997) Cellular solids: structure and properties. (2ndedn), Cambridge University Press. Cambridge.

11. Yannas IV (1995) Tissue regeneration templates based on collagen-glycosaminoglycan copolymers. Biopolymers 122: 219-244.

12. O'Brien FJ, Harley BA, Yannas IV, Gibson LJ (2005) The effect of pore size on cell adhesion in collagen-GAG scaffolds. Biomaterials 26: 433-441.

13. Gosline J, Lillie M, Carrington E, Guerette P, Ortlepp C, et al. (2002) Elastic Proteins: Biological Roles and Mechanical Properties. Philosophical Transactions: Biological Sciences 357: 121-132.

14. Redaelli A, Vesentini S, Soncini M, Vena P, Mantero S, et al. (2003) Possible role of decorin glycosaminoglycans in fibril to fibril force transfer in relative mature tendons--a computational study from molecular to microstructural level. J Biomech 36: 1555-1569.

15. Merryman WD, Huang HY, Schoen FJ, Sacks MS (2006) The effects of cellular contraction on aortic valve leaflet flexural stiffness. J Biomech 39: 88-96.

16. Harley BA, Leung JH, Silva EC, Gibson LJ (2007) Mechanical characterization of collagen-glycosaminoglycan scaffolds. Acta Biomater 3: 463-474.

17. Tilley JM, Chaudhury S, Hakimi O, Carr AJ, Czernuszka JT (2012) Tenocyte proliferation on collagen scaffolds protects against degradation and improves scaffold properties. J Mater Sci Mater Med 23: 823-833.

18. Tuckwell D, Humphries M (1996) Integrin-collagen binding. Semin Cell Dev Biol 7: 649-657.

19. Wissink MJ, Beernink R, Pieper JS, Poot AA, Engbers GH, et al. (2001) Binding and release of basic fibroblast growth factor from heparinized collagen matrices. Biomaterials 22: 2291-2292.

20. Sugahara K, Mikami T, Uyama T, Mizuguchi S, Nomura K, et al. (2003) Recent advances in the structural biology of chondroitin sulfate and dermatan sulfate. Curr Opin Struct Biol 3: 612-620.

21. Hubbell JA (2003) Materials as morphogenetic guides in tissue engineering. Curr Opin Biotechnol 14: 551-558.

22. Ferdous Z, Grande-Allen KJ (2007) Utility and control of proteoglycans in tissue engineering. Tissue eng 13: 1893-1904.

23. Uygun BE, Stojsih SE, Matthew HW (2009) Effects of immobilized glycosaminoglycans on the proliferation and differentiation of mesenchymal stem cells. Tissue Eng Part A 15: 3499-3512.

24. Waterhouse A, Wise SG, Ng MK, Weiss AS (2011) Elastin as a Nonthrombogenic Biomaterial. Tissue Eng Part B Rev 17: 93-99.

25. Karnik SK, Brooke BS, Bayes-Genis A, Sorensen L, Wythe JD, et al. (2003) A critical role for elastin signaling in vascular morphogenesis and disease. Development 130: 411-423.

26. Rnjak-Kovacina J, Wise SG, Li Z, Maitz PK, Young CJ, et al. (2012) Electrospun synthetic human elastin: collagen composite scaffolds for dermal tissue engineering. Acta Biomater 8: 3714-3722.

27. Dreger SA, Thomas P, Sachlos E, Chester AH, Czernuszka JT, et al. (2006) Potential for Synthesis and Degradation of Extracellular Matrix Proteins by Valve Interstitial Cells Seeded onto Collagen Scaffolds. Tissue Eng 12: 2533-2540.

28. Taylor PM, Sachlos E, Dreger SA, Chester AH, Czernuszka JT, et al. (2006) Interaction of human valve interstitial cells with collagen matrices manufactured using rapid prototyping. Biomaterials 27: 2733-2737.

29. Colazzo F, Sarathchandra P, Smolenski RT, Chester AH, Tseng YT, et al. (2011) Extracellular matrix production by adipose-derived stem cells: Implications for heart valve tissue engineering. Biomaterials 32: 119-127.